



**HAL**  
open science

## Low-dose electron diffraction tomography (LD-EDT)

Stéphanie Kodjikian, Holger Klein

► **To cite this version:**

Stéphanie Kodjikian, Holger Klein. Low-dose electron diffraction tomography (LD-EDT). *Ultramicroscopy*, 2019, 200, pp.12-19. 10.1016/j.ultramic.2019.02.010 . hal-02017894

**HAL Id: hal-02017894**

**<https://hal.science/hal-02017894>**

Submitted on 21 Dec 2021

**HAL** is a multi-disciplinary open access archive for the deposit and dissemination of scientific research documents, whether they are published or not. The documents may come from teaching and research institutions in France or abroad, or from public or private research centers.

L'archive ouverte pluridisciplinaire **HAL**, est destinée au dépôt et à la diffusion de documents scientifiques de niveau recherche, publiés ou non, émanant des établissements d'enseignement et de recherche français ou étrangers, des laboratoires publics ou privés.



Distributed under a Creative Commons Attribution - NonCommercial 4.0 International License

# “Angular resolution expected from iCHORD orientation maps through a revisited ion channeling model”

C. Langlois<sup>1</sup>, T. Douillard<sup>1</sup>, S. Dubail<sup>2</sup>, C. Lafond<sup>1</sup>, S. Cazottes<sup>1</sup>, J. Silvent<sup>3</sup>, A. Delobbe<sup>3</sup>, P. Steyer<sup>1</sup>

<sup>1</sup>Université de Lyon, INSA-Lyon, MATEIS CNRS UMR5510, 7 avenue Jean Capelle, 69621 Villeurbanne (France)

<sup>2</sup>Axon Square SAS, 4 la Tuilière, 74140 Sciez (France)

<sup>3</sup>Orsay Physics, 95 Avenue des Monts Auréliens, 13710 Fuveau (France)

**Abstract:** Crystalline orientation maps are obtained in a Focused Ion Beam (FIB) microscope using the ion CHanneling ORientation Determination (iCHORD) method, which relies on the channeling phenomenon observed in ion-induced secondary electron images. The current paper focuses on the angular resolution that can be expected from such orientation maps, obtained using a revisited ion channeling model. A specific procedure was developed to evaluate the angular resolution, based on the distribution of orientation errors when evaluating controlled sample disorientation. The main advantage is that no external reference is required. An angular resolution of 1° is obtained on a nickel based sample using standard acquisition conditions. This value fulfills most of the needs in terms of microstructural characterization usually carried out by Electron Back Scattered Diffraction.

## 1. Introduction

Orientation mapping in a Scanning Electron Microscope (SEM) is now a common technique in academic and R&D laboratories through the Electron Back Scattered Diffraction (EBSD) technique. Useful information about crystallographic texture, strain localization and phase discrimination in samples of different natures (ceramics, metals, semiconductors, geological samples) are accessible. The requirements in terms of spatial resolution, angular resolution, and acquisition speed usually depend on the type of issue to be addressed. For local texture studies, statistical data are needed on a large number of grains, which means a high acquisition speed, whereas the angular resolution has not to be better than ~1°. A fast acquisition will also be necessary when covering a large area of a sample, which is particularly true for geological samples <sup>[1]</sup>, or during *in situ* tests <sup>[2]</sup> and 3D acquisitions <sup>[3]</sup>. On the contrary, local strain characterization requires very high angular and spatial resolutions <sup>[4]</sup>. In this context, it is interesting to propose appropriate approaches to address these different materials science topics. For the EBSD technique, recent models of camera allow for either

high speed or high quality Kikuchi pattern acquisitions <sup>[5]</sup>. Apart from the camera, other acquisition configurations inside the microscope are proposed like off- or on-axis Transmission Kikuchi Diffraction (TKD) <sup>[6,7]</sup>, which is adapted for thin samples in transmission mode and gives a better spatial resolution.

The Kikuchi diffraction is not the only way to obtain orientation maps on a polycrystalline bulk sample. The channeling contrast visible on images acquired using an ion beam in a Focused Ion Beam (FIB) microscope also contains crystallographic information that can be used to map the orientations without using an extra detector or a dedicated camera. The proof-of-concept and the *modus operandi* of this new method, called iCHORD for ion CHanneling ORientation Determination, is described in Langlois *et al.* <sup>[8]</sup>. Beyond the proof-of-concept, it is now crucial to determine the performance of iCHORD in terms of angular and spatial resolutions as well as acquisition/indexation speed in order to define potential targeted applications. In this work, the latests developments regarding the ion channeling model used in iCHORD are first exposed because it consists in the core of the iCHORD approach. The question of angular resolution measurement is then discussed and an original methodology suitable for iCHORD is proposed and applied on a standard iCHORD experiment.

## 2. Experimental details

All the experiments reported in this paper were carried out on a ZEISS NVision40 FIB-SEM instrument in order to obtain both ion-induced secondary electron images and EBSD orientation maps. The EBSD maps have been acquired with an Oxford Instruments™ F+ EBSD system (fast camera NordlysII and Channel 5 software). Concerning the ion source, the microscope is equipped with a SIINT Zeta column and a Ga liquid metal ion source (Seiko Instruments Inc. NanoTechnology, Japan). A sample tilt of 40° was systematically chosen. Actually, the tilt value must be high enough to allow the ion beam crossing several crystallographic planes, as explained in Langlois *et al.* <sup>[8]</sup>. Considering the chosen sample tilt and magnification, no dynamic focus was necessary. Conditions used for ion-induced secondary electron imaging on a texture-free copper sample were: 30 kV, beam current of 700 pA, pixel size of 110 nm and a dwell time of 120 ns. A series of 180 images (dimension 2048 x 1536 ; angular step 2°) was acquired in ~40 min resulting in an orientation map of dimension 1324 x 1372 pixels with a field of view of 145 μm. This set of data was used to illustrate the ion channeling model presented Section 3.

To determine quantitatively the angular resolution, a texture-free nickel alloy sample (Inconel 718) was used. Acceleration voltage and probe current were respectively equal to 30 kV and 1.5 nA, with a magnification of 600x, which corresponds to a pixel size of 93 nm. A complete rotation of 360°

was carried out in 60 min using an angular step of 2°. For each rotation step, two images were acquired, one with a dwell time of 1.6 µs per pixel, and a second one with a shorter dwell time equal to 0.12 µs. All the images with a dwell time of 1.6 µs constitute the image series #1 whereas all the images acquired with a dwell time of 0.12 µs constitute the image series #2. Raw image dimensions are 2048 x 1536 pixels, corresponding to a field of view of width 190 µm. After mutual image alignment, the two image series are reduced to dimensions 1320 x 1224 pixels (field of view of width 123 µm), mainly due to the fact that the scan rotation is not corrected during the sample rotation. For all the calculations related to the angular resolution determination exposed in Section 5, six-binned versions (without averaging) of the two Inconel image series were used to limit the computation time.

For the acquisition of these different images series, ion currents up to 1.5 nA were used considering the good resistance of copper and nickel toward ion sputtering.

### 3. Modeling the ion channeling

To compute a theoretical intensity profile for a given orientation of the crystal, Langlois *et al.* <sup>[8]</sup> have used a model based on crystallographic calculations involving a lot of parameters to be manually set to properly fit the experimental intensity profiles. In the present work, a more numerical approach is used, based literally on the principle of “ballistic channeling” of incident particles. To date, this approach has been tested only for cubic structures, and the adaptation for other crystallographic systems is in progress.

Atomic positions are first generated for the cubic crystal of interest in the form of an array  $A$  containing atom coordinates as well as atom type. For most cases, a volume of 6 x 6 x 6 unit cells is enough for the calculations, centered on the origin of the coordinates frame. At the beginning of the modelization process, the crystal axes are aligned with the orthonormal reference frame of the microscope with the ion beam parallel to  $\vec{e}_z$ . Since we want to compute a theoretical intensity profile for a crystal with an orientation defined by its three Euler angles  $(\varphi_1, \phi, \varphi_2)$  in the Bunge’s convention, the atomic positions are first rotated according to the active orientation matrix  $M$  defined by <sup>[9]</sup>:

$$M = \begin{pmatrix} \cos \varphi_2 \cdot \cos \varphi_1 - \sin \varphi_2 \cdot \cos \phi \cdot \sin \varphi_1 & -\cos \varphi_2 \cdot \sin \varphi_1 - \sin \varphi_2 \cdot \cos \phi \cdot \cos \varphi_1 & \sin \varphi_2 \cdot \sin \phi \\ \sin \varphi_2 \cdot \cos \varphi_1 + \cos \varphi_2 \cdot \cos \phi \cdot \sin \varphi_1 & -\sin \varphi_2 \cdot \sin \varphi_1 + \cos \varphi_2 \cdot \cos \phi \cdot \cos \varphi_1 & -\cos \varphi_2 \cdot \sin \phi \\ \sin \phi \cdot \sin \varphi_1 & \sin \phi \cdot \cos \varphi_1 & \cos \phi \end{pmatrix}$$

Euler angles  $(\varphi_1, \phi, \varphi_2)$  represent the orientation of the crystal that would be found in an EBSD map. A new array  $A'$  now contains the updated atomic positions  $A'_i$  given by:

$$A'_i = M \cdot A_i$$

defined in the microscope reference frame. In the iCHORD acquisition setup (see Figure 1. of Langlois *et al.* <sup>[8]</sup>), the sample is tilted around the  $\vec{e}_x$  axis at a constant angle of  $\psi = 40^\circ$ , and rotated around the tilted rotation axis with an angular step  $\Delta\theta$  until a complete turn is achieved, which means  $N = (360/\Delta\theta)$  rotations. It is then necessary to compute the array  $A''$  containing the atomic positions for a given rotation step, in order to calculate the corresponding intensity level.

### 3.1. Orientation matrix of the crystal during the acquisition procedure

At the beginning of the acquisition process, the direction perpendicular to the sample surface is along  $\vec{e}_z$ . The initial operation is a tilt around  $\vec{e}_x$  at a constant angle of  $\psi = 40^\circ$ . The corresponding active rotation matrix is given by:

$$T_\psi = \begin{pmatrix} 1 & 0 & 0 \\ 0 & \cos \psi & -\sin \psi \\ 0 & \sin \psi & \cos \psi \end{pmatrix}$$

Then, the sample is rotated around its tilted surface normal direction. For each rotation step, the atomic positions are left-multiplied by an active matrix  $R_{\Delta\theta}$  corresponding to a rotation of  $\Delta\theta$

around the tilted rotation axis  $\vec{t} = T_\psi \cdot \vec{e}_z = \begin{pmatrix} 0 \\ -\sin \psi \\ \cos \psi \end{pmatrix}$ . The matrix  $R_{\Delta\theta}$  is defined using the formulae

that yields the active rotation matrix corresponding to the axis-angle pair  $(\vec{t}, \Delta\theta)$  <sup>[9]</sup>:

$$R_{\Delta\theta} = \begin{pmatrix} \cos \Delta\theta & -\cos \psi \cdot \sin \Delta\theta & -\sin \psi \cdot \sin \Delta\theta \\ \cos \psi \cdot \sin \Delta\theta & \cos \Delta\theta + \sin^2 \psi (1 - \cos \Delta\theta) & -\sin \psi \cdot \cos \psi (1 - \cos \Delta\theta) \\ \sin \psi \cdot \sin \Delta\theta & -\sin \psi \cdot \cos \psi (1 - \cos \Delta\theta) & \cos \Delta\theta + \cos^2 \psi (1 - \cos \Delta\theta) \end{pmatrix}$$

After  $p$  rotation steps, the atomic positions  $A''_i$  stored in array  $A''$  are obtained by:

$$A''_i = (R_{\Delta\theta})^p \cdot T_{\psi=40^\circ} \cdot A'_i$$

Once the atomic positions are computed for this rotation state, the question becomes: how to determine the intensity received by the detector?

### 3.2. Intensity simulation

According to the ballistic description of the channeling effect <sup>[10]</sup>, if interplanar spaces are available for the ion beam to travel in, the intensity will be low because the secondary electron emission will be generated too deep under the surface, so that most of electrons do not reach the surface and then the detector. To simulate this effect, an algorithm has been developed, fully detailed in Appendix A and briefly described hereafter to clarify several choices made to avoid simulation artefacts. To compute the intensity value at a given rotation state, atomic positions contained in array  $A''$  are projected onto a plane perpendicular to the ion beam (so, perpendicular to  $\vec{e}_z$ ). To avoid projection artefacts, only the atomic positions contained in a sphere of radius equal to 3 unit cells and centered on the origin are projected. The choice of a sphere is justified by less projection artifacts: the area on which the atoms are projected is constant for all orientations and rotation steps, which is not the case if the full 6 x 6 x 6 unit cells parallelepiped is projected. Atoms have their respective atomic radius and they project themselves orthogonally as discs in the projection plane, which is tangent to the sphere. To take into account the decreasing interactions between the ion beam and the atom as a function of the depth, a brightness value in the range 0-255 is associated to each atom (and each discs in the projection plane) following a decreasing function of type  $G(d) = a \cdot d^b$  (see Figure 1a and 1b) with  $d$  the distance between the atom and the projection plane. When parts of discs overlap on the projection plane, the part which belongs to the atom with the smallest distance to the projection plane has the priority to give its brightness in the projection. An example of such projection is presented in Figure 1b.

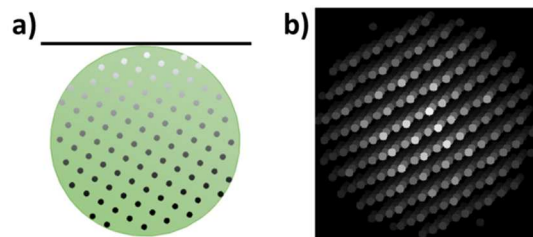


**Figure 1.** Computation of the intensity in a given orientation during the rotation series acquisition. a) Atomic brightness as a function of the distance toward the projection plane represented by the black line on the top; b) Projection plane on which atoms are projected in the form of disks of different brightness levels.

After the projection, let us consider now the sum of the brightness values  $s_i$  for all the pixels  $i$  constituting the projection plane:

$$S = \sum_i s_i$$

In the projection plane, the channeling condition corresponds to low values for  $S$  because, for instance in the extreme case of a low index zone axis, a complete row of atoms will project itself onto one single disc, leaving a large area with brightness levels equal to zero. On the contrary, in non-channeling conditions, most of the pixels of the projection plane will have non-zero brightness levels, resulting in high values for  $S$ . Due to this strong correlation, the value  $S$  is associated to the theoretical intensity value for this rotation step. A complete intensity profile is obtained by repeating the intensity calculation for each rotation step. At the end of the process, if it helps to obtain a better fit with the experimental intensity profiles, the theoretical intensity profiles are raised to a power between 1 and 5. All the theoretical and experimental profiles are normalized by dividing each value of a profile by its norm.

### 3.3. Adjustment of the parameters

As already mentioned, a sphere radius equals to 3 unit cells is enough to model the channeling effect in the projection plane. Other parameters to be adjusted in the simulation are the size of the projection in pixels, the atomic radii, the value of the decay factor 'a', value of decay power 'b' for the function  $G(d)$  and the power on the output profile. For the size of the square projection area (in pixels), a default value limiting the calculation time while keeping reasonable fidelity compared to experimental values is 8 times the diameter of the sphere with a one-to-one correspondence between Angströms and pixels. For example, for copper with lattice parameter  $a = 3.615$  angstroms, the diameter of the sphere is  $D_{sphere} = 6 \cdot a$  so the square projection size will be  $48 \cdot a = 175$  pixels. Atom radii can be chosen following different models (atomic-ionic radii <sup>[11]</sup> and crystal radii <sup>[12]</sup>) according to the structure studied, with eventually a scaling factor that applies on all radii. Standard parameters are: decay factor 'a' equal to 3, decay power 'b' equal to 4 and an output power equal to 2. After a first run with these standard parameters and a small database (i.e. 200k profiles), a coarse orientation is found, that is used to refine the parameters. Then, a complete database is computed. This work has to be done only once for each material and iCHORD acquisition configuration (tilt angle and high tension). Once the database is computed, it can be used for any experimental data acquired in the same conditions with the same materials.

### 3.4 Application example on copper sample

In order to evaluate the model, it is necessary to measure how close theoretical and experimental profiles are, for a representative set of known orientations. To achieve this comparison, an iCHORD acquisition has been performed on a polycrystalline copper sample without any marked texture (Figure 2a). An EBSD map was also acquired on the same area, in order to obtain the Euler angles at each position from which theoretical profiles can be computed (Figure 2b). The “distance” between experimental (E) and theoretical (T) profiles obtained at the same position is expressed with the following formula:

$$\text{distance} = 1 - E \cdot T$$

with profiles E and T considered as two vectors of same dimension to compute their dot product. Using this formula, two profiles are very close if their associated distance is close to zero. The distance map for each position of the region of interest is presented Figure 2c, together with the distribution of these distances (Figure 2d). The distances between the experimental and theoretical profiles are close to zero throughout the area, with a narrow distribution peaked at 0.005. It is obviously not the case at grain boundaries and positions corresponding to dust on the sample surface. It is worth mentioning that the sample is not textured, so that many random orientations are represented in the region of interest. It means that the developed model computes theoretical profiles with high fidelity whatever the orientation. These results have been confirmed on several other cubic materials such as TiN<sup>[8]</sup>, Co and Ni superalloys<sup>[13]</sup>, Al and Fe.

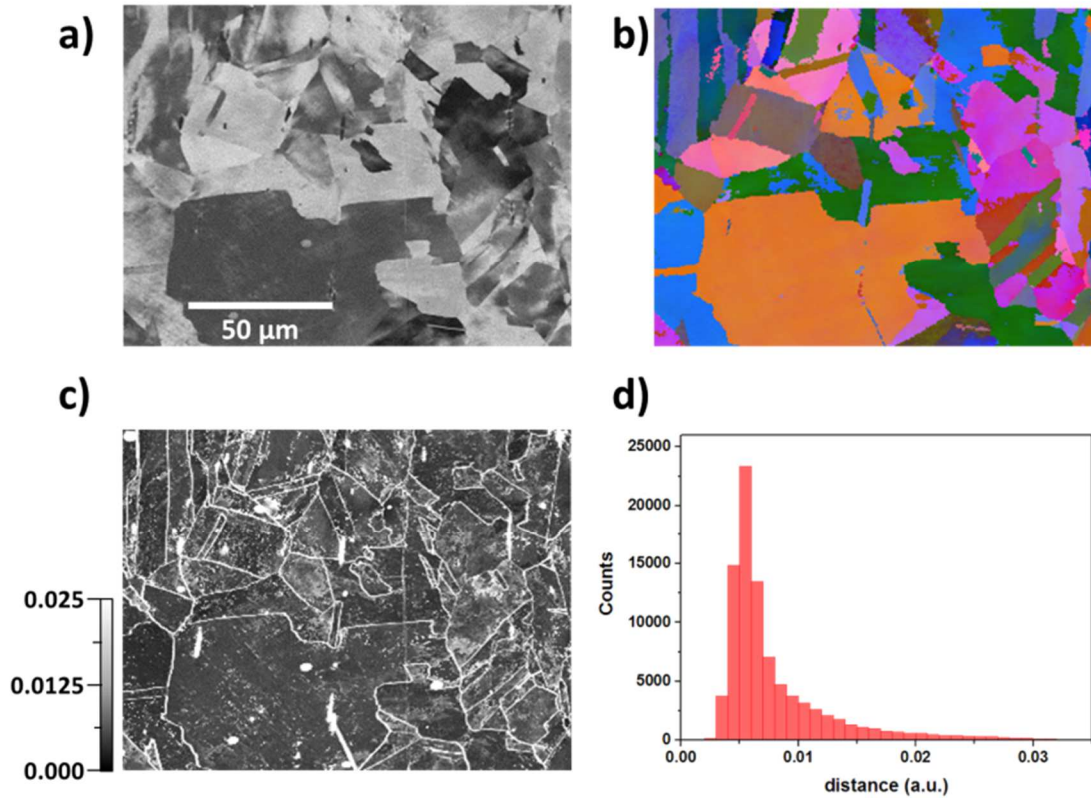


**Figure 2.** Evaluation of the ion channeling model on a copper sample. a) image extracted from the ion image series, b) denoised EBSD Euler map on the same area aligned with the ion image series, c) map of the “distance” (see text for the definition of “distance” in this context) between experimental and theoretical profiles for each orientation in the region of interest, d) distribution of the ‘distance’ map values. White pixels on c) represent distances equal or superior to 0.025.

To help the reader visualizing the agreement between theoretical and experimental profiles, Figure 3 gathers on the same plot theoretical and experimental profiles extracted from a position in the ion image series corresponding to Euler angles  $(162.35^\circ \ 28.94^\circ \ 2.47^\circ)$ . This position has been chosen because the distance between the two profiles is 0.0055, which is the peak value of the ‘distance’ distribution presented Figure 2d. It means that, globally, the agreement presented for this specific orientation is representative of the situation for other orientations.

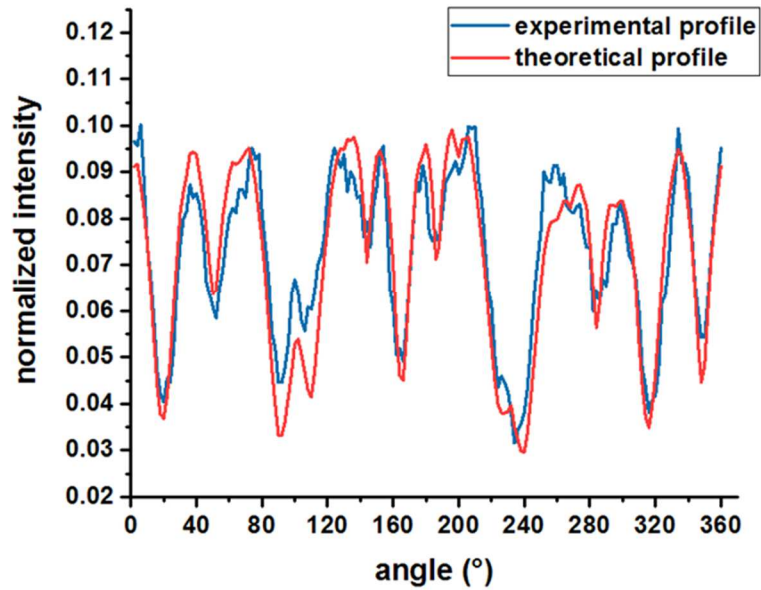


**Figure 3.** Representative example of correspondence between experimental and theoretical profiles for the Euler triplet  $(162.35^\circ \ 28.94^\circ \ 2.47^\circ)$ . The distance between the two profiles is 0.005, which is the most frequent distance between experimental and theoretical profiles in the tested area on copper sample.

## 4. Robustness of the revisited ion channeling model toward orientation indexation

### 4.1. Relationship between distance and disorientation for two theoretical profiles

The central question for orientation mapping is the ability to distinguish between two very close orientations from their signatures, which are their experimental profiles in the iCHORD approach. The signature differences must be related to the disorientation between these two close orientations. This relationship cannot be precisely evaluated experimentally because the orientations are initially not known. Using EBSD would be useless because of the different acquisition geometry leading to orientation errors and spatial distortions as well as the very large amount of experimental data that would be necessary to sample experimentally the orientation space. However, the analysis can be carried out at least theoretically, shedding light on the relationship between orientation and intensity profiles.

The first step of the analysis is to generate a set of 100 000 random orientations in the fundamental zone corresponding to the cubic system. For each orientation of this set, a theoretical profile (vector of 180 components) is computed using the model exposed in Section 3. Then, among this orientation set, 5 000 pairs of orientations are selected with the condition that their disorientation is under  $3^\circ$  because the focus is on the separation between close orientations. More

precisely, to construct such pairs, an orientation is selected with its theoretical profile, and a search of the best match is performed in the set of 100 000 profiles. Because the orientation set is small (100k orientations only), the disorientation corresponding to this match is distributed between 0° and 3°, which corresponds to the intended analysis. For more details concerning the construction and use of such random orientation set, see Appendix B.

Figure 4 shows a graph with disorientation as a function of the distance. Each pair (distance ; disorientation) previously computed is represented by a red data point. In order to illustrate the influence of the database size on the distance and disorientation ranges, the same analysis has been carried out using datasets of 250 000, 500 000 and 1 000 000 profiles, and results have been added also on Figure 4 (see the figure caption of associated colors).

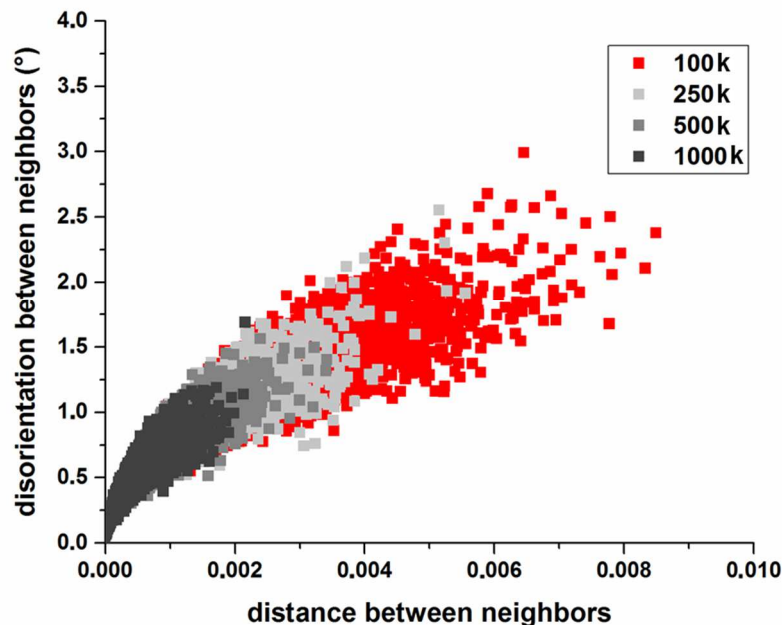


**Figure 4.** *Disorientation as a function of the distance for pairs of orientations. Results using different dataset sizes are presented.*

It appears that the relationship linking the distance between pairs and their disorientation is not linear. It is worth noting that for a given distance, the possible disorientation interval is bounded, and that this interval is converging toward low values when the distance decreases down to zero, which is the fundamental core of the indexing procedure, described in Appendix C. It can be concluded that the distance between profiles is a pertinent indicator of the disorientation for small distance values. However, one can expect slightly lower experimental performance compared to the results of this purely theoretical analysis. As an illustration, let us recall the results from Section 3.4 on copper sample, for which the distance between an experimental profile and a theoretical profile